THE AMERICAN SOCIETY OF MECHANICAL ENGINEERS
345 E. 47 St., New York, N.Y. 10017

85-DET-145

Critical Speeds of TurboMachinery: Computer Predictions vs. Experimental Measurements PART I: The Rotor Mass—Elastic Model

by

J. M. VANCE
Professor of Mechanical Engineering
Texas A&M University

B. T. MURPHY
Technical Staff Member
Rocketdyne Corporation

H. A. TRIPP
Staff Research Engineer
Shell Development Company

ABSTRACT

This is the first part (Part I) of two papers describing results of a research program directed at verifying computer programs used to calculate critical speeds of turbomachinery. This research program was undertaken since questions existed about the accuracy of calculations for the second and higher critical speeds.

Part I describes improvements in computer programs and data modeling that resulted from comparing measured and calculated "free-free" natural frequencies of several shafts and rotors. Program modifications to improve accuracy include consideration of the effect of disk/shaft attachment stiffness, revised treatment of the end masses, and an improved convergence. Modifications resulting from this study are applicable to many other damped and undamped critical speed computer programs.

INTRODUCTION

Continuing demand for increased performance of modern turbomachinery in the petroleum industry has resulted in machines being designed for operation at speeds approaching the second critical speed. In fact, machines have been purchased and delivered which operated so near a critical speed that difficulty was encountered in maintaining acceptable rotor balance.

Since most machines purchased for petrochemical and natural gas service are custom-designed for a particular application, the problem described above cannot be solved by standardizing mass-produced components.

Requirements for accurate critical speed prediction capabilities are thus indicated. The acceptable margin between the critical speed and the operating speed depends on the desired margin and on the error in the calculations. For example, if operating speeds are not to be within fifteen percent of any critical speed, and the error in critical speed prediction is plus or minus five percent, then the specified margin must be twenty percent.

Literature describing experimental verification of existing critical speed computer programs is almost nonexistent. In most cases where predicted and measured critical speeds are compared, it is for a purpose other than verifying the analysis. In fact, input data (i.e. the rotor-bearing physical parameters) are sometimes adjusted as required to obtain the best agreement with measured results. An example is reference (1), where the average discrepancy between the measured and computed (before adjustment) first two natural frequencies of four rotors was 7%, and 14%, respectively. In cases where the relative effects of varying design parameters are being investigated, the adjustment of parameters to produce a baseline case is completely justified. For prediction of critical speeds during a machine design phase, these parameter adjustments can only be made by a program user who has had extensive experience with actual machines.

Initial measurements indicated significant differences between measured and calculated critical speeds of a laboratory rotor/bearing apparatus. In order to eliminate the bearing parameters and foundation effects, the "free-free" natural frequencies of the rotor were measured. Significant differences between these measured values and frequencies calculated using state-of-the-art damped and undamped computer programs led to the first part of this investigation, which was directed at verifying the equations used by the computer programs for calculating rotor natural frequencies. This was done by comparing computer predictions with experimentally measured "free-free" natural frequencies of selected shafts and rotors. In Part II, state-of-the-art computations are compared with measurements from rotors operating in fluid-film bearings.

It should be understood that the rotor "free-free" mode shapes and natural frequencies do not directly correspond to critical speeds of rotors in actual machines. The first two rotor critical speeds in many machines are rigid body modes that do not have corresponding "free-free" natural frequencies. The first bending "free-free" natural frequency can be compared with the first actual bending mode of the rotor-bearing system only if the bearings are extremely flexible.

Presented at the ASME Design Engineering Division Conference and Exhibit on Mechanical Vibration and Noise
Cincinnati, Ohio—September 10-13, 1985

However, the "free-free" natural frequencies and mode shapes are an excellent way of checking the accuracy of the rotor mass-elastic model without involving uncertainties of the bearing parameters. It is interesting to note that the mass-elastic model can contain large errors without introducing significant errors of the computed first critical speeds of many machines. In fact, the first critical speed of a machine with a very stiff rotor can be calculated by using the total rotor mass and the bearing stiffness. Furthermore, as shown in reference (2), the first measured critical speed of a flexible rotor in fluid film bearings can be frequently calculated by assuming the rotor is on rigid simple supports. Consequently, good agreement between the calculated and measured values of the first critical speed on bearings is not necessarily an indicator that the mass-elastic model is accurate or that the critical speeds of the higher modes will be accurately predicted.

UNDAMPED CRITICAL SPEED COMPUTER PROGRAM

Most computer programs for calculating critical speeds of rotating machinery are based on the transfer matrix method. The method was developed concurrently and independently in the 1940's by Myklestad, for calculating natural frequencies of airplane wings, and by Prohl, for calculating critical speeds of steam turbines. In its modern form, it has been adapted for high speed digital computers, and is especially well suited for personal computers.

Most versions of the transfer matrix type program ignore damping (which is often small) in order to simplify the calculations. For the work described here (Part I), a program without damping is justified since the "free-free" modes of vibration involve very little damping. Programs which do include damping are usually based on the recent work of Lund (2), and have the capability to predict rotordynamic instability as well as damped critical speeds. These programs use the same mass-elastic models as undamped computer programs, but do require computer algorithms involving complex numbers. Such a program was written for Part II of this work.

Refinements and modifications to improve the accuracy of the critical speed calculations resulted from "free-free" natural frequency measurements made on a number of different shafts and rotors of varying complexity.

EXPERIMENTAL METHODS AND PROCEDURES

In making the experimental measurements of natural frequencies for "free-free" supported shafts and rotors, the methods and equipment described below were found to improve the repeatability and accuracy of the data obtained:

Rotor Support

Figure 1 shows the type of rotor support that was found to work best for measuring "free-free" frequencies. With the rotor hung horizontally from two long wires or ropes, the vibration excitation was applied in the horizontal plane. This resulted in a pendular (horizontal) stiffness of each wire support of:

$$K_H = W/2\ell \qquad (1)$$

where W was the weight of the rotor and ℓ was the length of each wire support in inches.

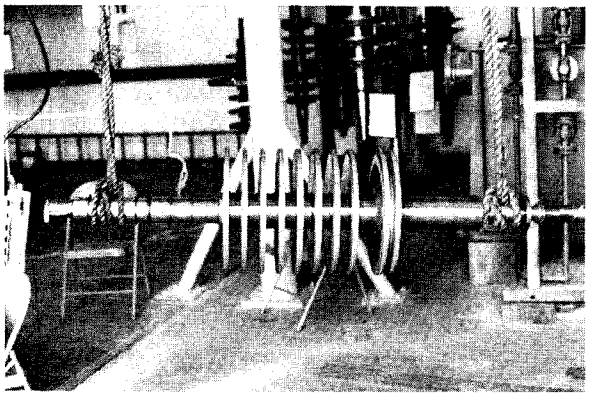

Figure 1. Steam Turbine Rotor Suspended by Ropes for "Free-Free" Vibration Measurements

As long as the support ropes were longer than 1/3 the length of the rotors, they were found to have a negligible effect on the measurements.

Excitation Methods

Random (white noise), impact (using a rubber or plastic hammer), and to a lesser extent, sinusoidal vibration excitation were all used in the experiments.

Random and impact excitations were found to produce comparable results, but the impact method required more time and work since a large number of averages was required. The disadvantage of random excitation was that a white noise generator was needed and a suitable shaker had to be attached to the rotor.

Sinusoidal excitation was best suited to cases where only one frequency or mode was investigated, since the signal generator could be tuned to the natural frequency of interest.

Experimental Techniques

Small accelerometers, each weighing 2.7 grams, were used for measuring "free-free" shaft and rotor natural frequency mode shapes. Similar measurements using non-contacting proximity probes showed that attaching the accelerometers to the shafts did not have a measurable effect on the natural frequencies or the mode shapes.

For natural frequency measurements, an accelerometer was mounted on one end of the rotor and the accelerometer signal was analyzed using a spectrum analyzer. Initial measurements produced a spectrum with a broad frequency range that was used to identify the first four or five natural frequencies. Additional measurements utilized the "zoom expansion" feature of the analyzer to measure each of the identified frequencies using high resolution (narrow bandwidth). Early in the project, it was found that failure to use a narrow bandwidth resulted in errors as high as four percent.

Mode shapes were obtained by using an FFT analyzer to measure the transfer function between two accelerometers mounted on the rotor. One accelerometer mounted at one end of the rotor was used as a reference, and the other accelerometer was used to define the mode shape at points along the rotor. To maximize the accuracy of the mode shape measurements, the two accelerometers were calibrated

simultaneously, and the coherence function was measured along with each transfer function measurement. In almost all of the mode shape measurements, the transfer function phase angle was found to vary less than 3 degrees from 0° or 180°, which indicated little damping within the rotor.

Rotor dimensions, used to generate accurate computer models, were obtained by taking micrometer measurements of the rotor outer diameter at various axial locations along the shaft and at all disks and other changes in diameter. These measurements were accurate to ±.03mm (±.001"). Axial measurements (e.g. rotor length) were taken with steel rules and were accurate to ±.8mm (±1/32").

The rotors were weighed, which together with the dimension measurements confirmed the density of 7830 kg/m^3 (.283 lb/in^3) used in the computer models.

PROGRAM AND MODELING MODIFICATIONS

Five areas were investigated while attempting to improve agreement between the calculated and measured "free-free" natural frequencies. These areas are addressed individually in the order they were investigated. Thus, calculations shown in any area include corrections that have been previously covered. Where applicable, typical experimental results are shown, illustrating the effect described.

All the shafts and rotors tested were made of steel. A Young's modulus of 207 GP (30.0 x 10^6 psi) was used in the calculations.

Convergence Criterion. All critical speed programs of the type described here generate numerical elements d_{ij} of the transfer matrix defined by

$$\begin{bmatrix} M_R \\ V_R \end{bmatrix} = \begin{bmatrix} d_{11} & d_{12} \\ d_{21} & d_{22} \end{bmatrix} \begin{bmatrix} \theta_L \\ X_L \end{bmatrix} \qquad (2)$$

where M_R, V_R are the moment and shear at the right end of the rotor, and θ_L, X_L are the displacements at the left end.

The d_{ij} are functions of frequency. The computer algorithm finds the natural frequencies ω which make the determinant $D(\omega)$ of the matrix D_{ij} as close to zero as possible. One commonly used criterion for success is for $|D| \leq \varepsilon$, where ε is a small predetermined number. If the criterion is not satisfied, an improved estimate for the frequency is calculated using a Newton-Raphson scheme:

$$\omega = \omega_o - D_o(\omega_o - \omega_1)/(D_o - D_1) \qquad (3)$$

where ω_o, D_o are the most recent values of frequency and determinant.

ω_1, D_1 are previous values of frequency and determinant.

ω is the new estimate for natural frequency.

As D_o gets smaller, the difference between ω_o and ω_1 also becomes smaller. However, an acceptable value of D_o for one rotor, or for one mode, will often produce unacceptable inaccuracy (in ω) for another rotor or mode.

This source of error was eliminated by implementing a convergence criterion based on $(\omega_o - \omega_1)$ rather than the criterion based on D_o.

A comparison of measured "free-free" and calculated natural frequencies for a uniform shaft with only minute changes in station diameter are given in Table 1. The two sets of calculated natural frequencies were obtained using the same program with the determinant convergence criterion and then the frequency convergence criterion. The percent error between the measured and calculated frequencies are given in parenthesis. This illustrates the significant improvement in accuracy that resulted by using the frequency convergence criterion.

Table 1. "FREE-FREE" NATURAL FREQUENCIES OF A UNIFORM SHAFT, .0762m (3.025") IN DIAMETER X 1.278m (50.33") LONG

Measured	Computed Using Determinant Convergence Criterion	Computed Using Frequency Convergence Criterion
212.5	206.1 (-3.01)	210.9 (-0.75)
581.2	630.9 (8.55)	567.4 (-2.37)
1106.2	1145.6 (3.56)	1077.5 (-2.59)
1775.0	1888.1 (6.37)	1714.8 (-3.39)

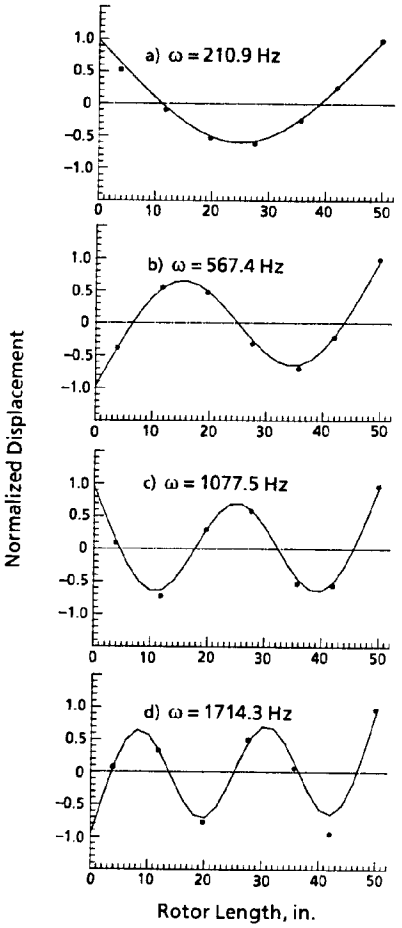

Figure 2. A Comparison of Measured and Calculated "Free-Free" Mode Shapes of a 3 Inch Diameter Shaft, 50.33 Inches Long
Measurements are indicated by the data points and calculated mode shapes are indicated by the solid lines

06044

Figure 2 shows the calculated mode shapes for each frequency, with the measured deflections plotted as data points.

Effect of Concentrated End Masses Due to the Definition of Rotor Stations in the Transfer Matrix Model. Figure 3 shows the transfer matrix model for a uniform shaft with only four stations (three segments). As usual, the last station on the right has zero length.

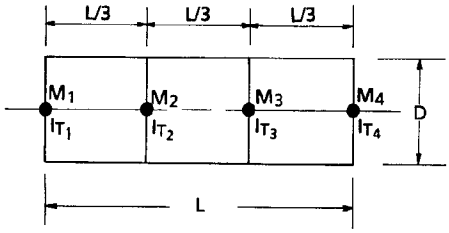

Figure 3. Transfer Matrix Model for Uniform Shaft

A typical convention for lumping mass properties is for each station to use one-half of the mass and mass moment of inertia of the shaft segments to the left and right of the station. This gives:

$$m_1 = m_4 = \bar{\rho}L/6,$$

$$m_2 = m_3 = \bar{\rho}L/3,$$

where $\bar{\rho}$ is the mass/unit length.

Similarly,

$$I_{T_1} = I_{T_4} = \frac{\bar{\rho}L}{6}\left(\frac{D^2}{16} + \frac{L^2}{108}\right)$$

and

$$I_{T_2} = I_{T_3} = \frac{\bar{\rho}L}{3}\left(\frac{D^2}{16} + \frac{L^2}{108}\right),$$

where moments of inertia are taken about the centroids of the segments.

Using the values above to calculate the total mass and moment of inertia for the shaft gives

$$M = \sum_1^4 m_i = \bar{\rho}L \qquad (4)$$

which is correct, and

$$I_T = \sum_1^4 I_{T_i} + 2\,m_2\,(\tfrac{L}{6})^2 + 2m_1\,(\tfrac{L}{2})^2 = \bar{\rho}L\left(\frac{D^2}{16} + \frac{L^2}{9}\right),$$

which is incorrect, since the correct moment of inertia for the shaft is

$$I_T = \bar{\rho}L\left(\frac{D^2}{16} + \frac{L^2}{12}\right). \qquad (5)$$

The difference results from m_1 and m_4 being further from the center of gravity of the shaft than they should be.

A correction factor f was derived to transfer part of the end mass to the next inboard station. Using the left end station as an example, the corrected lumped masses m'_1 and m'_2 are

$$m'_1 = fm_1 \qquad (6)$$

$$m'_2 = m_2 + (1-f)m_1 \qquad (7)$$

$$f = \frac{1}{1+\ell/4a}, \qquad (8)$$

where

ℓ = $\ell_1 + \ell_2$ (the length of segments 1 and 2)

a = distance from station 2 to the center of gravity of the rotor.

Using $\ell_1 \approx \ell_2$, and $a \approx L/2$ f was approximated by

$$f = \frac{1}{1 + \ell_1/L} \qquad (9)$$

Using the incorrect moment of inertia caused significant errors in the calculated natural frequencies when a small number of stations were used and for shafts with large masses near the ends. For the tests discussed here, the rotors were well defined and this correction to the end masses improved the program accuracy by less than one percent.

Effect of Shear Deflection. In most turbomachinery, practically all of the shaft deflection is due to bending. However, for short, large diameter shafts and shafts with large overhung disks, shear deflection can have a significant effect on calculated critical speeds.

Critical speed programs currently available use several different equations for calculating shear effects. Among the equations checked, the equation which most accurately modeled the shear deflection measured in a test shaft was the one developed by Timoshenko and used by Lund (2). The transfer equation for deflection due to both bending M and shear V is

$$X_{n+1} = X_n + \ell_n\theta_n + \left(\frac{\ell_n^2}{2EI}\right)M_n + \frac{\ell_n^3}{6EI}V_n - \frac{1.33\,\ell_n}{A_nG}V_n \qquad (10)$$

with the last term representing Timoshenko's shear deflection effect.

Measurements were made on a short .2921m (11-1/2") large diameter .1524m (6") shaft in order to determine the error associated with shear deflection effects.

Table 2 shows shear deflection in this shaft was quite significant. The RMS error for the first three modes was reduced from 33.6% without shear to 2.0% when shear was included for a 24 station model.

Table 2. "FREE-FREE" NATURAL FREQUENCIES OF A UNIFORM SHAFT, .1524m (6") DIAMETER X .2921m (11-1/2") LONG

Measured	Computed (% error) 24 Stations	
Hz	w/shear effect	no shear effect
5252	5292 (+0.8)	5829 (+11.0)
9700	9540 (-1.6)	12947 (+33.5)
14489	14063 (-2.9)	21217 (+46.4)
Overall RMS Error:	2.0%	33.6%

Some interesting observations were made when making the experimental measurements on this shaft. The measured frequencies were quite sensitive to the measurement technique. For example, the natural frequency at 9700 Hz disappeared completely when one particular combination of shaker and random noise generator was used. These types of anomalies were not

observed in the measurement on longer shafts and rotors.

The effect of the improved convergence criterion, treatment of end masses, and including shear deflection calculations, can be illustrated by comparing measured and calculated "free-free" natural frequencies for the laboratory apparatus rotor shown in Figure 4. This rotor had three large disks, but was machined from one piece of stock to eliminate uncertainty about the effects of attachments or interfaces. The rotor weighed 168.kg (370. lb), and was 1.33m (52.4") long. The disks' diameters were .2527m (9.95 inch) O.D. by .127m (5.00 inch) long and were spaced on .254m (10") centers.

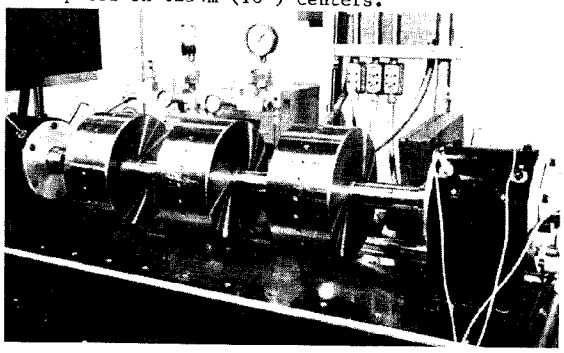

Figure 4. Three-Disk Lab Rotor Installed on Tilting-Pad Bearings

Table 4 gives the measured and computed natural frequencies and the error in percent for the three-disk rotor. The attachment stiffness of the .127m (5") thick disks was so high that disk flexibility did not make a significant difference between the two results. Figure 5 shows the computed mode shapes for each natural frequency, with the measured modal deflections plotted as individual points. The computed mode shapes included the flexible disk effect.

Table 4. "FREE-FREE" NATURAL FREQUENCIES FOR THREE-DISK LAB ROTOR

Measured	Computed	
	Modified Program	Original Program
Hz	Hz (% error)	Hz (% error)
94	95 (+1.1)	102.2 (8.7)
207	207 (0)	200 (-3.38)
356	353 (-0.8)	345.3 (-3.0)
463	408 (-11.9)	613.7 (32.5)
832	850 (+2.2)	
1037	968 (-6.7)	

Effect of Exterior Disks

In order to determine the effect a pressed on disk or sleeve has on the calculations, a uniform shaft with a hydraulically press-fitted disk was assembled. The rotor was 50.8mm (2") in diameter by 1.224m (48-3/16") long. The disk was .2286m (9") in diameter by 76.2mm (3") long.

Table 5 gives the measured natural frequencies and natural frequencies calculated using integral disk and external mass models, along with the error in percent. In this particular case, larger errors were

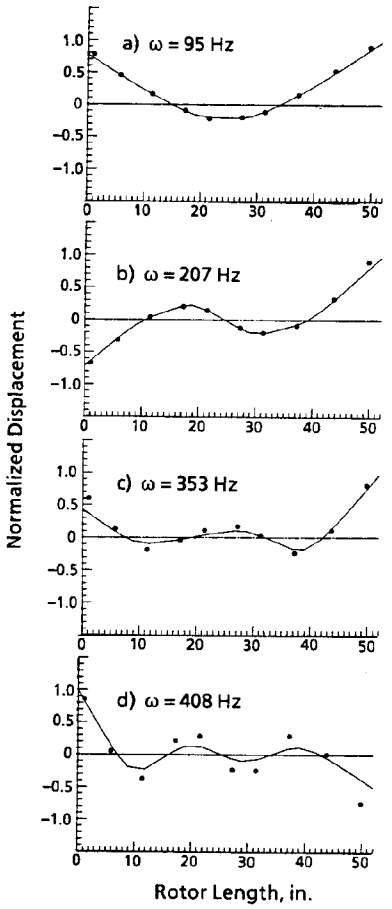

Figure 5. A Comparison of Measured and Calculated "Free-Free" Mode Shapes of the 3-Disk Rotor
Measurements are indicated by the data points and calculated mode shapes are indicated by the solid lines

present when the disk was treated as an exterior mass rather than as an integral part of the shaft.

Table 5. "FREE-FREE" NATURAL FREQUENCIES OF A UNIFORM SHAFT WITH A SINGLE MASSIVE DISK

Measured	Disk as an Integral Part of Shaft	Disk as an External Mass
Hz		
130.76	133.2 (+1.87)	121.8 (- 6.85)
356.64	355.3 (-0.37)	366.2 (+ 2.68)
632.65	632.0 (-0.10)	714.9 (+13.00)
1132.80	1137.0 (+0.37)	1096.9 (- 3.17)

These results are similar to those previously published (5). In this reference, the interference fit on a test rotor was found to have a major effect on the stiffness of a non-rotating rotor and to offer no stiffness for rotational speeds above 3500 rpm.

Effect of Disk/Shaft Attachment Flexibility. One of the usual assumptions in critical speed analysis is that shaft disk and wheels remain rigid and do not deform as the shaft vibrates. A further assumption is

that the attachment of the disks to the shaft is also rigid, so that the disks remain normal to the neutral axis of the shaft. Recently these assumptions have been questioned (3).

In this present work, one additional degree of freedom for each disk was introduced to calculate the effect of flexibility in the attachment of disks to the shaft, as shown in Figure 6. The local shaft slope θ differs from the angular disk deflection θ' of the disk by the amount α, as a result of a finite moment stiffness of the attachment, K_T (inch/lb/radian).

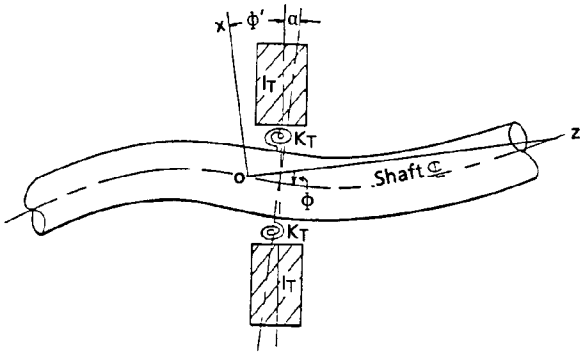

Figure 6. Effect of Disk Attachment Flexibility

Analysis of the dynamic effect was based on mechanical mobility and impedance considerations. By definition, the impedance of the rigid disk is:

$$Z_d = \frac{M}{\theta} = -I_T \omega^2, \qquad (11)$$

where ω is the frequency of the local exciting moment M.

For a rigid attachment, the moment transferred across the n^{th} disk in the computer program is

$$M_{n+1} = M_n + Z_{dn}\theta_n \qquad (12)$$
$$= M_n - I_{Tn}\omega^2\theta_n$$

For a flexible attachment, the moment stiffness K_T is in series with the inertia I_T. The resulting modified impedance of the disk is

$$Z_d = \frac{1}{\bar{M}_K + \bar{M}_I}, \qquad (13)$$

where $M_K = \frac{1}{K_T}$ and $\bar{M}_I = \frac{-1}{I_T\omega^2}$

are the mobilities of the disk attachment stiffness and inertia respectively.

Thus,

$$Z_d = \frac{-K_T I_T \omega^2}{K_T - I_T\omega^2}, \qquad (14)$$

and the new transfer equation for the n^{th} disk is

$$M_{n+1} = M_n + Z_{d_n}\theta_n \qquad (15)$$
$$= M_n - \frac{K_T I_T \omega^2}{K_T - I_T\omega^2}\theta_n$$

To utilize equation (15) in the program, a numerical value for the attachment stiffness K_T was required. Calculations of this stiffness were based on an equation from the theory of elasticity, given in reference (4) which considers the bending of the disk itself.

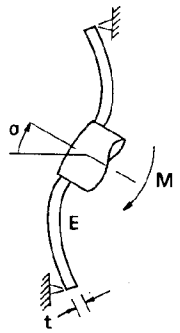

$$\sigma = \frac{M}{\alpha E t^3}\,\alpha = \alpha(r_o/a)$$

$$\text{So } K_T = \frac{M}{\sigma} = \alpha E t^3 \sim \frac{\text{in.-lb}}{\text{rad.}}$$

E = Young's modulus, PA (psi)
t = Disk thickness, m (in.)
μ = Poisson's ratio
r_o = Shaft radius, m (in.)
a = Radius of the disk, m (in.)
α = Shape factor

Figure 7. Formula for Disk Attachment Stiffness K_T
From Roark, R. J., Formulas for Stress and Strain McGraw-Hill, 4th Edition, NY, 1965, p. 242

Figure 7 shows the model, the equation, and the shape parameter α used to calculate the attachment stiffness. A quadratic equation used in the computer program to define the shape factor α, and the resulting curve are shown in Figure 8.

Experimental measurements of the attachment stiffness for several rotor disks showed good agreement with results calculated using this method.

Extensive laboratory measurements made on a 119kg rotor from a single-stage steam turbine illustrate the effect of disk/shaft attachment flexibility. This rotor was characterized by a single turbine disk that was much larger in diameter than the shaft. Table 6 gives measured natural frequencies and natural frequencies calculated with and without disk/shaft attachment included, with the percent error for each case given in parenthesis. Note that without the disk flexibility effect, the third measured mode was completely missed.

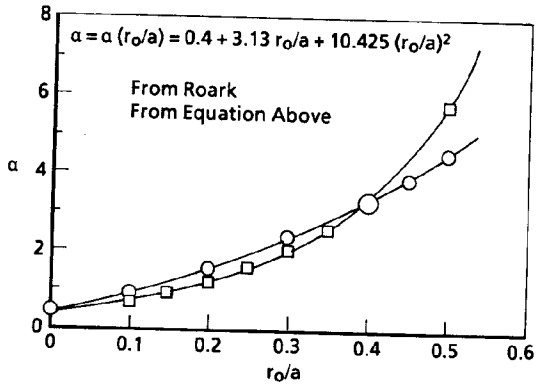

Figure 8. Shape Factor α for $K_T = \alpha Et^3$

Table 6. "FREE-FREE NATURAL FREQUENCIES OF A SINGLE-STAGE STEAM TURBINE ROTOR"

Measured	Computed	
	No Flexible Disk	W/Flexible Disk
Hz	Hz (% error)	Hz (% error)
373	376 (+0.8)	376 (+0.8)
602	622 (+3.3)	603 (+0.2)
1033	No (∞)	907 (-12.2)
1262	1219 (-3.4)	1230 (-2.5)
1998	1642 (-17.8)	1795 (-10.2)
2509	2321 (-7.5)	2410 (-3.9)

The computed mode shapes (with the disk flexibility correction) for this rotor are shown as solid lines in Figure 9, with the measured modal deflections plotted as data points. Good agreement exists, especially for the first two modes.

The second and third mode shapes have a node at the turbine disk and appear to be very similar. Detailed accelerometer measurements were made on and near the turbine disk to determine differences between the two modes. The node of the second mode (602 Hz) was found to be located very near the centerline of the disk, and the pitching motion of the disk was in phase with the oscillating slope of the shaft at the disk. The node of the third mode (1033 Hz) was located near the inside face of the turbine disk, and the pitching motion of the disk and slope of the shaft at the disk were out of phase. (The phase of these disk modes is illustrated by the dashed lines on Figures 9-b and 9-c.) The third mode could not be computed without using the disk flexibility option in the program.

RESULTS USING INDUSTRIAL ROTORS

To determine the accuracy of the modified computer program, measurements for several compressor and turbine rotors were compared with calculated "free-free" natural frequencies.

Three spare replacement rotors for typical refinery compressors were tested at the rotor storage facility. Each was suspended in a horizontal position by ropes from a crane and excited in the horizontal plane by a nylon hammer. Frequency analysis of the rotor response was used to measure the natural frequencies.

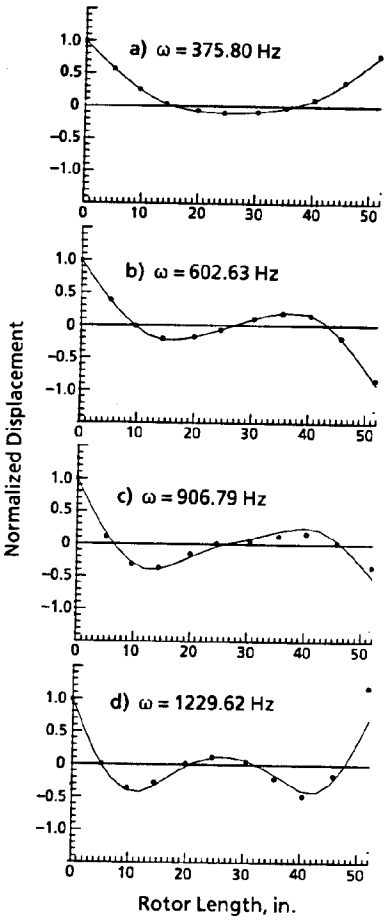

Figure 9. A Comparison of Measured and Calculated "Free-Free" Mode Shapes for a Single Stream Turbine Measurements are indicated by the data points and calculated mode shapes are indicated by the solid lines

Computed natural frequencies for three compressor rotors are compared to the measured frequencies in Tables 7, 8 and 9. The three calculated sets of natural frequencies for each rotor are:

1. From rotor station data as supplied by the manufacturer.
2. From the data in (1) but as modified by actual dimensional measurements.
3. From the same data as (2), using the "flexible disk" option in the computer program.

The percent error for each case is shown in parenthesis.

The large errors associated with the first set of calculations were due mainly to deficiencies in the rotor data supplied by the manufacturer. Specifically, the manufacturer treated both the impeller wheels and spacer sleeves (between the impellers) as added weights. Neither the mass moment of inertia of the impellers nor the added shaft stiffness due to the sleeves could be computed from the data supplied.

Although these omissions partially cancelled each other's effect, the net resulted in a large difference between the measured and calculated natural frequencies.

To improve the rotor model data, the impeller and sleeve diameters were measured and used to modify the section diameters. As shown in the second column of computed results, these modifications reduce the error by a factor of almost two.

Table 7. "FREE-FREE" NATURAL FREQUENCIES OF A SIX-STAGE COMPRESSOR ROTOR

Measured from data Hz	Computed (% error) w/disk I_T as received	% sleeve O.D.'s	w/flexible disks
106	87 (-17.9%)	102 (-3.8%)	108 (+ 1.9%)
197	178 (- 9.6%)	192 (-2.5%)	196 (- 0.5%)
269	277 (- 3.0%)	294 (+9.3%)	303 (+12.6%)

Table 8. "FREE-FREE" NATURAL FREQUENCIES OF AN EIGHT STAGE COMPRESSOR ROTOR #1

Measured Hz	Computed (% error) from data as received	w/disk I_T % sleeve O.D.'s	w/floppy disks
60	39 (-35.0%)	58 (-3.3%)	58 (+3.3%)
142	99 (-30.33%)	130 (-8.5%)	155 (-9.2%)
240	189 (-21.3%)	222 (+7.5%)	243 (+1.3%)

Table 9. "FREE-FREE" NATURAL FREQUENCIES OF AN EIGHT STAGE COMPRESSOR ROTOR #2

Measured Hz	Computed (% error) from data as received	w/disk I_T % sleeve O.D.'s	w/flexible disks
84	69 (-17.9%)	88 (- 4.8%)	88 (+ 4.8%)
165	131 (-20.6%)	173 (- 4.8%)	172 (+ 4.2%)
241	178 (-26.1%)	267 (+10.8%)	267 (+10.8%)
322	264 (-18.0%)	382 (+18.6%)	404 (+20.3%)

A 13 stage steam turbine rotor, for use in the same compressor train as the three compressor rotors, was also tested in the same way as the compressor rotors.

The computed natural frequencies in Table 10 are based on rotor data supplied by the manufacturer, which included all of the outer diameters of the wheels and shaft sections. The two cases under the "computed" heading for this rotor are for rigid and flexible disk attachments.

In this case, the flexible disk attachments did not significantly improve the calculated natural frequencies.

Table 10. "FREE-FREE" NATURAL FREQUENCIES OF 13 STAGE STEAM TURBINE MOTOR

Measured Hz	Computed (% error) w/rigid disks	w/flexible disks
141	135 (- 4.3%)	135 (- 4.3%)
284	297 (+ 4.6%)	289 (+ 1.8%)
388	454 (+17.0%)	309 (-20.4%)
509	612 (+20.2%)	425 (-16.5%)
Overall error	RMS = 13.6%	RMS = 13.3%

CONCLUSIONS

The following conclusions resulted from the work discussed in Part I of this project:

1. Using a convergence criterion based on differences in frequency rather than on the matrix determinant significantly reduced the error in calculating natural frequencies.
2. Revising the treatment of the masses at the end stations marginally improved accuracy. For rotor station models consisting of only a few stations or for rotors with large masses near the shaft ends, this correction may be larger.
3. The shear deflection equation developed by Timoshenko was found to accurately model shear deformation in a shaft.
4. Disks, wheels and spacer sleeves were found to have a major stiffening effect on the measured "free-free" natural frequencies. For the rotors tested, the most accurate natural frequencies were calculated using station data that ignored the interface and used stiffnesses and inertias based on the outer diameters of pressed on sleeves and wheels. This effect is [illegible] not as pronounced in rotating machinery, but must be considered in "free-free" measurements.
5. The flexible disk effect is likely to be significant when disks or wheels with diameters more than twice the shaft diameter are located near a vibration node point. The flexible disk/shaft attachment has the effect of slightly lowering the existing computed natural frequency and introducing a new natural frequency, at a higher frequency, to account for the disk pitching (out of phase) on the shaft.

REFERENCES

1. Thomas, G. B. and Littlewood, P., "A Technique for Modeling Rotors from Measured Vibration Characteristics", Proceedings of the 2nd International Conference on Vibrations in Rotating Machinery, Cambridge, England, September 2-4, 1980, Institution of Mechanical Engineers, pp. 445-451.
2. Lund, J. W., "Stability and Damped Critical Speeds of a Flexible Rotor in Fluid-Film Bearings", ASME Journal of Engineering for Industry, May 1974, pp. 509-517.
3. Dopkin, J. A. and Shoup, T. E., "Rotor Resonant Speed Reduction Caused by Flexibility of Disks", Journal of Engineering for Industry, November, 1974, pp. 1328-1333.
4. Roark, T. J., Formulas for Stress and Strain, 4th Edition, McGraw-Hill, NY, 1965, p. 242.
5. V. Ya. Kal'mens: "The Effect of the Fitting of Discs and Bushings on Bending and Critical Velocity of a Turbine Rotor" Energomashinostroenie, No. 4, (1964), pp. 28-30.